Journal of Medicinal Chemistry

Article

pubs.acs.org/jmc

Mapping Selective Inhibition of the Cancer-Related Carbonic Anhydrase IX Using Structure−Activity Relationships of Glucosyl-Based Sulfamates

Brian P. Mahon,[†] Carrie L. Lomelino,[†] Janina Ladwig,[‡] Gregory M. Rankin,[‡] Jenna M. Driscoll,[†] Antonieta L. Salguero,[†] Melissa A. Pinard,[†] Daniela Vullo,[§] Claudiu T. Supuran,[§] Sally-Ann Poulsen,[‡] and Robert McKenna*[,†]

[†]Department of Biochemistry and Molecular Biology, College of Medicine, University of Florida, 1600 SW Archer Road, PO Box 100245, Gainesville, Florida 32610, United States

[‡]Eskitis Institute for Drug Discovery, Griffith University, Nathan, Queensland 4111, Australia

[§]Polo Scientifico, Neurofarba Department and Laboratorio di Chimica Bioinorganica, Università degli Studi di Firenze, Rm. 188, Via della Lastruccia 3, 50019 Sesto Fiorentino, Florence, Italy

Supporting Information

ABSTRACT: Inhibition of human carbonic anhydrase IX (hCA IX) has shown to be therapeutically advantageous for treating many types of highly aggressive cancers. However, designing selective inhibitors for hCA IX has been difficult due to its high structural homology and sequence similarity with off-target hCAs. Recently, the use of glucosyl sulfamate inhibitors has shown promise as selective inhibitors for hCA IX. In this study, we present five X-ray crystal structures, determined to a resolution of 1.7 Å or better, of both hCA II (a ubiquitous CA) and an engineered hCA IX-mimic in complex with selected glucosyl sulfamates and structurally rationalize mechanisms for hCA IX selectivity. Results from this study have allowed us, for the first time, to empirically "map" key interactions of the hCA IX active site in order to establish parameters needed to design novel hCA IX selective inhibitors.

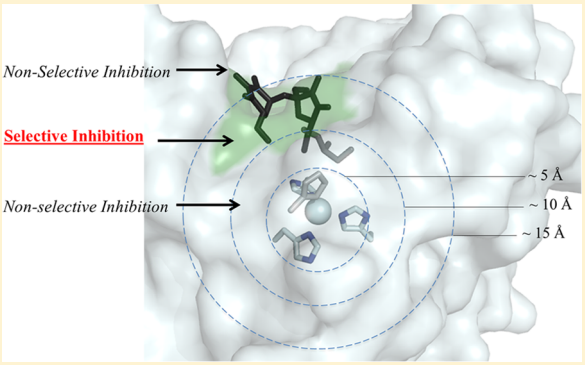

INTRODUCTION

Hypoxia in solid tumors is a condition commonly associated with metastatic transitions in tumor cells.[1,2] This hypoxic phenotype in tumor cells results in an outgrowth of their blood supply, leading to microenvironmental changes consisting of low oxygen concentration (typically ≤1% of overall oxygen content) and a decrease in extracellular pH (~pH 6.5).[1] This induces the tumor cells to transition their general metabolism from mitochondrial oxidative phosphorylation to glycolysis often independent of the amount of available O_2, a phenomenon described as the Warburg effect.[3,4] As a result of this glycolytic shift, there is an upregulation of pH homeostasis factors in tumor cells to establish a regulated intracellular/extracellular pH gradient.[5,6] One pH regulatory factor that is ubiquitous to hypoxic tumor cells is human carbonic anhydrase IX (hCA IX).[6,7] hCA IX has shown to be a critical enzyme for tumor cell survival and proliferation due to its role in maintaining a close-to physiological intracellular pH in tumor cells.[6,8] As such, inhibition of hCA IX activity in hypoxic tumor cells has proven to be detrimental to the cells growth and proliferation.[7,9−11]

hCA IX is a zinc metalloenzyme that catalyzes the reaction between carbon dioxide and water to produce bicarbonate and a proton. hCA IX is a homodimer, type 1 transmembrane enzyme with an extracellular catalytic domain, considered the primary "druggable" site.[12,13] While the expression of hCA IX is primarily limited to the stomach and GI tract in healthy tissue, hCA IX expression has been shown to be highly upregulated in multiple neoplastic tissue types.[6,7] Therefore, hCA IX is used as a prognostic marker for several cancer types.[14−16] Because of hCA IX's pivotal role in pH regulation in several tumors, its limited expression in normal human tissue, and its highly drug-targetable extracellular catalytic domain, hCA IX has been defined as an excellent drug target.[7,9,17]

While clinically used inhibitors of hCA currently exist, these are isoform nonspecific and may result in the inhibition of ubiquitously expressed CAs (such as hCA I and II) and could result in unwanted side effects.[18] Therefore, isoform specific hCA IX inhibitors are required. hCA IX inhibitor development is complicated by the fact that the 15 CA isoforms share a

Received: June 2, 2015
Published: July 23, 2015

DOI: 10.1021/acs.jmedchem.5b00845
J. Med. Chem. 2015, 58, 6630−6638

conserved active site architecture with limited sequence variation between residues.[19,20] However, isoform selectivity among hCA inhibitors has been shown to be feasible by utilizing structural information on the active sites, and a method termed the "tail approach," whereby inhibitors are designed utilizing a chemical group that coordinates to the active site zinc (zinc-binding group, ZBG) conjugated to a variable "tail" region designed to interact with residues toward the surface of the active site (discussed in detail by Pinard et al.[19]).

We have previously shown that a series of glucosyl sulfamates, where the sulfamate acts as a ZBG and the glucose or acetylglucose group acts as the "tail" (Figure 1), are excellent

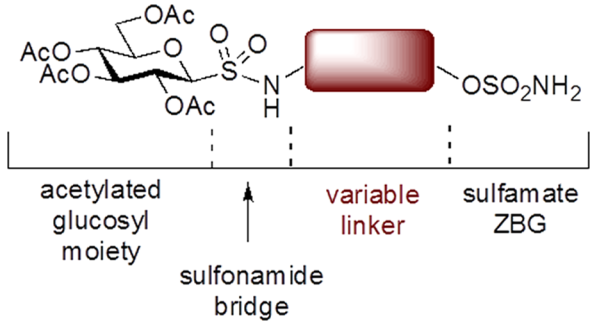

Figure 1. Schematic outlining the rational design of glucosyl sulfamate inhibitors. The general construct shows the primary sulfamate ZBG is conjugated to an acetylated glucosyl moiety and sulfonamide bridge by a variable linker region (highlighted in maroon).

hCA IX inhibitors that show capabilities to inhibit the enzyme better than off-target CA isoforms (hCA I and II) and also show limited membrane permeability allowing for location specific targeting of the extracellular hCA IX over other cytosolic hCAs. In addition, we have previously speculated on structure−activity (SAR) and structure−property relationships of these inhibitors with the active site of hCA IX and hCA II to rationalize their inhibition selectivity profiles.[21] In this study, we continue to study this series of hCA IX inhibitors to, for the first time, empirically "map" regions of selectivity in the hCA IX active site to determine key properties an inhibitor must exhibit in order to be isoform selective. To do this, we have solved five crystal structures of both wild-type hCA II and an engineered hCA IX-mimic (a molecule of hCA II with active site substitutions (hCA II numbering used throughout this manuscript) A65S, N67Q, E69T, I91L, F131V, K170E, and L204A to "mimic" hCA IX[21]) in complex with three inhibitors, denoted **623**, **625**, and **626** from the previously published glycoconjugate sulfamate series (see Moeker et al.[21]), all to a resolution of 1.7 Å or better. Results from this study will guide hCA IX selective inhibitor design and aide in the development of drugs that target the enzyme to treat several cancers.

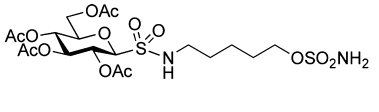

623

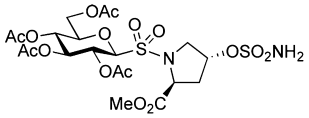

625

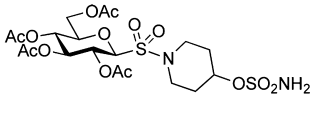

626

RESULTS AND DISCUSSION

Compound Design and Synthesis. The glucose-based sulfamate compounds are nonclassical hCA inhibitors as they comprise a primary sulfamate and not a primary sulfonamide as the zinc binding group (ZBG). Our group has had substantial success in developing hCA IX inhibitors through the combination of the sulfamate ZBG with a carbohydrate motif.[21] The acetylated glucose moiety is common to compounds **623**, **625**, and **626**; the glucose moiety is attached via a sulfonamide functionality to a variable linker region that terminates with the primary sulfamate ZBG. The linker length, steric bulk, and stereochemistry differ, with a *n*-pentyl chain **623**, pyrrolidine ring **625**, and piperidine ring **626** selected to probe potential differential hCA active site interactions with hCA II and IX.

The synthetic approach toward the acetylated carbohydrate-based sulfamates **623**, **625**, and **626** has been fully described by us earlier.[21,22] The synthesis proceeds in three steps commencing from reaction of 2,3,4,6-tetra-*O*-acetyl-1-*S*-acetyl-1-thio-*β*-D-glucopyranose with the corresponding amino alcohol, followed by oxidation to the sulfonamide, and last, sulfamoylation of the terminal alcohol functionality to install the sulfamate ZBG of **623**, **625**, and **626** (Supporting Information Scheme 1).

Selective hCA IX Inhibition. Inhibition data for **623**, **625**, and **626**, and clinically used hCA inhibitor acetazolamide (AZM) with hCA IX, I, and II (main off-target reservoirs) and hCA XII (which has also been linked to cancer progression[8,16]) are summarized in Table 1. The selectivity ratios for inhibition of hCA IX and hCA XII over the ubiquitously expressed hCA I and hCA II are also presented in Table 1.

We have previously discussed the SARs of each of the compounds in this study extensively (see Moeker et al.).[21] In brief, all compounds showed weakest inhibition of hCA I compared to hCA II, hCA IX, and hCA XII, which is a common observation for reported primary sulfonamide and sulfamate compounds and is desirable as hCA I is considered a main off-target hCA.[19,21] For hCA II, hCA IX, and hCA XII, the SAR vary, however, there is still a favorable selectivity ratio for each compound in terms of hCA IX inhibition. In this case, the inhibition profile for all compounds appears to depend mostly on the linker, as it is presumed the acetylation sites are present in the glucose moieties of each compound making the "tail" region common for each. Observations of selectivity ratios indicate the use of a five-membered pyrrolidine ring system shows the highest selectivity (**625**, I/IX = 4750, II/IX = 360), followed by a six-membered piperidine ring system (**626**, I/IX = 1200, II/IX = 130), and the least selective being a linear pentyl linker (**623**, I/IX = 175, II/IX = 5). A similar trend in selectivity is seen with each compound's affinity for hCA XII. The rationale for utilizing acetylated glucosyl tail moieties allows for significant contributions to the compound's steric bulk as well as hydrogen bonding capacity of the "tail" moiety. As such, compounds **623**, **625**, and **626** are shown to be excellent hCA IX inhibitors, all with K_i values of 2 nM (Table 1). In addition to these attributes, it has been previously demonstrated that the in vitro metabolic stability, plasma stability, and plasma protein binding characteristics for the acetyl groups, when presented on a glucose scaffold, allows these compounds to exhibit properties of ester prodrugs.[23] However, as we will show, there is a significant deacetylation of each of the compounds by both hCA II and the hCA IX-mimic,

DOI: 10.1021/acs.jmedchem.5b00845
J. Med. Chem. 2015, 58, 6630−6638

Table 1. Inhibition and Isozyme Selectivity Ratio Data for Human CA Isozymes I, II, IX, and XII with Compounds 623, 625, and 626, and Clinically Used Acetazolamide (AZM)

	K_i (nM)[a]				selectivity ratio[b]			
compd	hCA I	hCA II	hCA IX	hCA XII	I/IX	II/IX	I/XII	II/XII
623	350	10	2	9	175	5	39	1
626	2400	265	2	60	1200	133	40	4
625	9500	725	2	1	4750	363	9500	725
AZM	250	12	25	6	10	0.5	42	2

[a]Errors in the range of ±5% of the reported value from three determinations. [b]Selectivity is determined by the ratio of K_is for hCA isozyme relative to hCA IX and XII.

Table 2. X-ray Crystallography Statistics for Data Processing and Refinement of Ligand Bound CAIX-Mimic and CA II Crystal Structures

	hCA IX-mimic:**623** 4ZWX	hCA IX-mimic:**625** 4ZWY	hCA IX-mimic:**626** 4ZWZ	hCA II:**623** 4ZX0	hCA II:**625** 4ZX1
space group			$P2_1$		
cell dimensions (Å; deg)			a = 42 ± 0.8, b = 42 ± 0.8, c = 72 ± 0.5; β = 104 ± 0.3		
resolution (Å)	19.8−1.70 (1.75−1.70)	19.8−1.61 (1.66−1.61)	19.9−1.55 (1.58−1.55)	32.0−1.50 (1.54−1.50)	20.0−1.60 (1.66−1.60)
total reflections	36753	36949	38399	38025	31556
R_{sym}[a] (%)	5.7 (57.3)	4.3 (64.4)	10.3 (62.9)	4.7 (32.1)	6.3 (41.3)
$I/\sigma(I)$	20.5 (1.74)	24.5 (1.56)	9.35 (0.38)	47.2 (5.31)	19.61 (2.91)
completeness (%)	93.3 (93.6)	89.1 (84.9)	98.4 (94.2)	98.2 (99.0)	97.8 (97.1)
R_{cryst}[b] (%)	16.0 (22.4)	16.1 (23.6)	15.7 (27.0)	15.5 (22.6)	15.2 (24.7)
R_{free}[c] (%)	19.2 (25.8)	21.1 (26.8)	19.5 (31.0)	17.3 (27.2)	17.8 (29.8)
no. of protein atoms	2094	2082	2081	2085	2064
no. of water molecules	199	232	264	285	296
no. of ligand atoms	37	28	28	31	31
Ramachandran stats (%): favored, allowed, outliers	96.9, 3.14, 0.0	96.1, 3.53, 0.39	96.9, 3.12, 0.0	96.5, 3.54, 0.0	97.2, 2.77, 0.0
av B factors (Å^2): main chain, side chain, solvent, ligand[d]	17.3, 21.3, 26.0, 27.5	18.3, 22.3, 47.5, 30.0	17.5, 21.5, 40.5, 31.7	20.5, 24.7, 42.9, 34.5	14.1, 18.6, 21.1, 28.6

[a]$R_{sym} = (\sum|I - \langle I\rangle|/\sum\langle I\rangle) \times 100$. [b]$R_{cryst} = (\sum|F_o - F_c|/\sum|F_o|) \times 100$. [c]$R_{free}$ is calculated in the same way as R_{cryst} except it is for data omitted from refinement (5% of reflections for all data sets). [d]Values in parentheses correspond to the highest resolution shell.

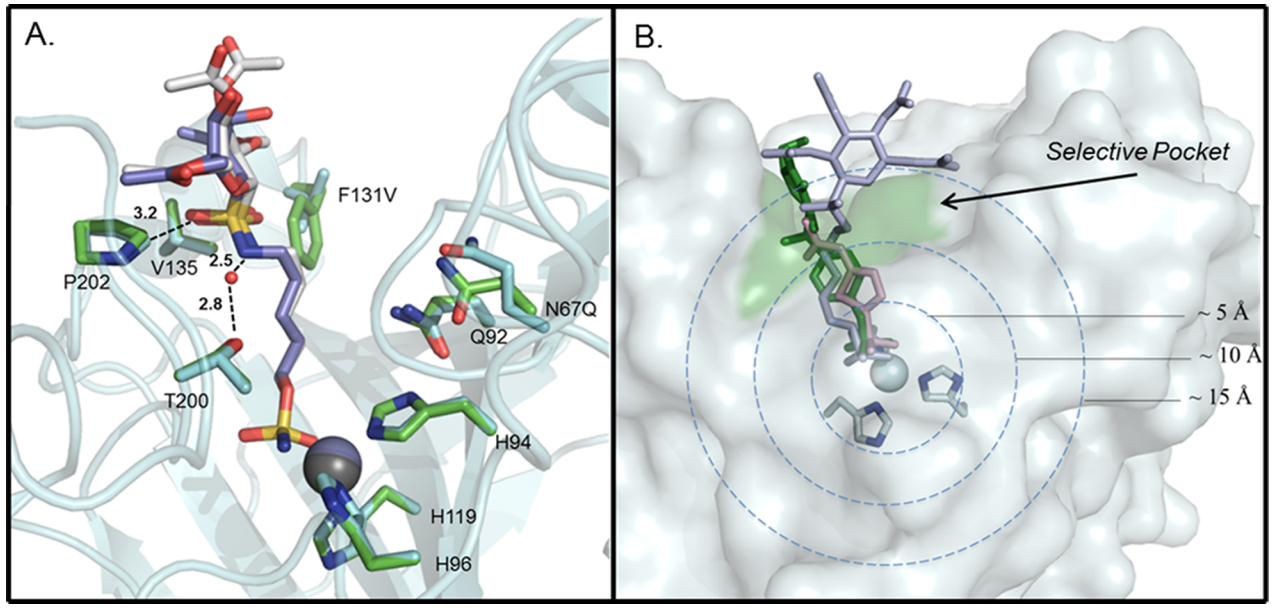

Figure 2. Compound **623** bound in the active site of both hCA II (green) and the hCA IX-mimic (cyan). (A) Overlay of the coordinates of compound **623** (shown as sticks, rmsd = 1.12 Å) from both hCA II (purple) and the hCA IX-mimic (white) with active site residues and relative bond distances (Å) labeled. Waters are shown as red spheres. (B) Cross-section of the hCA active site marking distance shells relative to the active site zinc. The *selective pocket* is highlighted in green, and overlays of compounds ranging in selectivity are shown as sticks. The least selective compounds (compounds **623**, gray, and AZM,[12] pink) and highly selective (compound **5d**, labeled as per Moeker et al.,[21] PDB ID 4RS9, green). Figure was made using PyMol.[38]

DOI: 10.1021/acs.jmedchem.5b00845
J. Med. Chem. 2015, 58, 6630−6638

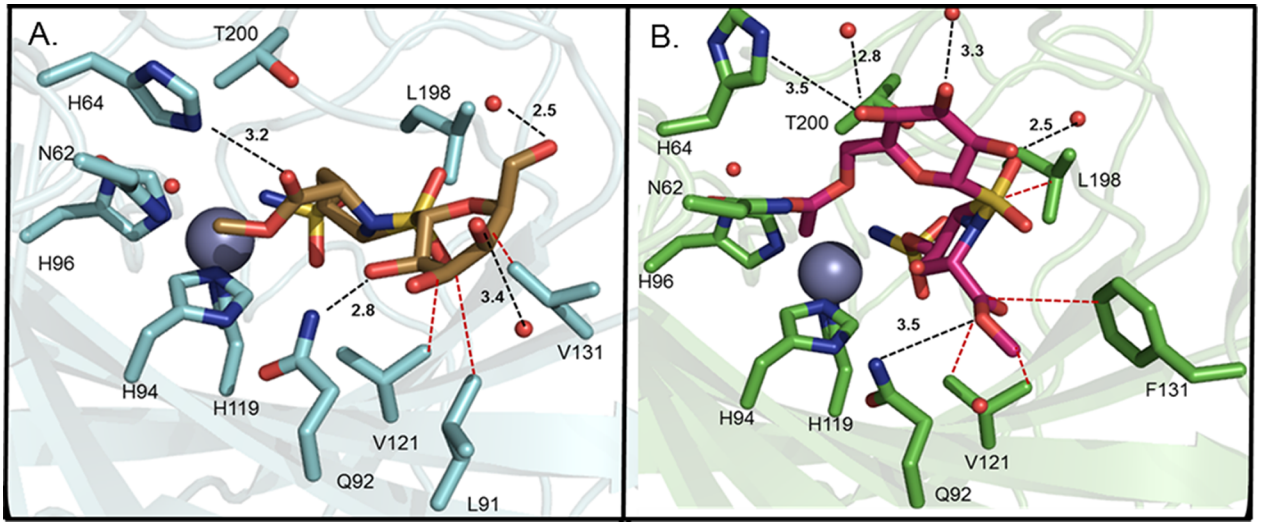

Figure 3. Compound **625** bound in the active site of both hCA II (green) and the hCA IX-mimic (cyan) with specific residues labeled. (A) Specific interactions of compound **625** (tan) with the active site of the hCA IX-mimic are shown with relative bond distances shown as black dotted lines with distances labeled (Å), hydrophobic interactions shown as red dotted lines, and water molecules shown as red spheres. (B) Specific interactions of compound **625** (pink) with the active site of the hCA II are with relative bond distances shown as black dotted lines with distances labeled (Å), hydrophobic interactions shown as red dotted lines, and water molecules shown as red spheres. Figure was made using PyMol.[38]

suggesting a possible "auto-unmasking" of these inhibitors during delivery (Supporting Information Figure S1). It should be noted, however, that this phenomenon has only been recorded in vitro and it is uncertain how this mechanism would affect these compounds in vivo.[24,25] As such, we will not emphasize in this study the in vitro mechanism of these compounds as we are unsure of its impact in vivo.

X-ray Crystallographic Results. X-ray crystallography (statistics summarized in Table 2) was used to analyze the mode of binding of compound **623** in complex with hCA II (K_i = 11 nM) and the hCA IX-mimic (hCA IX K_i = 2 nM) to gain insight in to the ∼5-fold selectivity (Table 1) of **623** for hCA IX. Structural analysis of the hCA IX-mimic in complex with **623** (Figure 2A) displays direct binding to the active-site zinc via the primary sulfamate group. Furthermore, binding of **623** causes an almost complete displacement of the ordered water network in the active site that has been determined important for catalysis.[26,27] The only water present in the enzymes active site is observed coordinated between the hydroxyl of the side chain of Thr200 and the NH of the sulfonamide linker of **623** (Figure 2A). The "tail" region of **623**, comprising the sulfamate-linked acetylated glucose moiety shows limited interaction with the hCA IX-mimic active site. Other primary interactions are observed occurring between the sulfonyl linker and Pro202 (Figure 2A). Comparisons of the binding modalities of compound **623** as it resides in the active site of hCA II show the interactions are mostly conserved (Figure 2A), with possible van der Waals (vdw) interactions only occurring between C1 of the acyl linker of **623** and Phe131. The conserved interactions between the hCA IX-mimic and hCA II correlates to the limited difference in K_i values between the hCA II and hCA IX (Table 1). In addition, cleavage of acyl groups (most likely through the weak esterase activity exhibit by hCA II, Figure S1) are observed, specifically on C2 and C3 of the glucose ring moiety (Supporting Information Figure S2A).[24] It is possible this esterase activity is more prevalent in hCA II, and the deacetylation of the glucose ring in compound **623** may contribute to the slight reduction in K_i value between hCA II and hCA IX, as glucose groups appear to bind unfavorably to the active site of hCA II.[21,28] It is also observed that compound **623** shows limited interaction in what has been defined as the *selective pocket* of the CA active site, or the region of the active site farthest from the catalytic zinc that contains residues that vary between isoforms (reviewed in detail by Pinard et al.[19] and Aggarwal, et. Al.[20]). The linear pentyl linker region of compound **623** causes the acetylated glucose group to extend ∼15 Å from the catalytic zinc, which induces an extension of this group out of the active site (Figure 2B). This essentially abolishes any interactions the "tail" region of compound **623** could form in the enzymes *selective pocket*. As such, the importance of this region in the CA active site is shown in Figure 2B, where the least selective compounds (in this case acetazolamide and compound **623**) form few or no interactions with residues in the *selective pocket* which is located between 10 and 15 Å away from the catalytic zinc. Alternatively, compounds that show high selectivity for hCA IX (such as compound **626′** from Moeker et al.,[21] Supporting Information Figure S1) have "tail" groups that interact directly in this region (Figure 2B).

X-ray crystal structures of compound **625** in complex with both hCA II and the hCA IX-mimic were determined (statistics summarized in Table 2). Compound **625** shows a higher selectivity (∼400-fold) for hCA IX over hCA II with K_i values of 2 and 740 nM, respectively (Table 1). Similar to compound **623**, compound **625** binds directly to the active site zinc in the hCA IX-mimic via the sulfamate moiety. In addition, the ordered water network shows complete displacement. Key interactions are observed via the five-membered pyrrolidine linker group with the side chain of His64 (proton-shuttling residue),[29] which further increases the compound's ability to abolish CA activity. In addition, a hydrogen bond is formed between the OH at position 2 of the glucose moiety with Gln92 (Figure 3A). The majority of interactions appear to be with hydrophobic residues in Val131, Leu91, and Val121 (Figure 3A). In addition, there are vdw interactions forming between the sulfonyl linker of compound **625** and Leu198. Comparatively, compound **625** binds in the active site of hCA II directly to the active site zinc via the sulfamate moiety and

DOI: 10.1021/acs.jmedchem.5b00845
J. Med. Chem. 2015, 58, 6630−6638

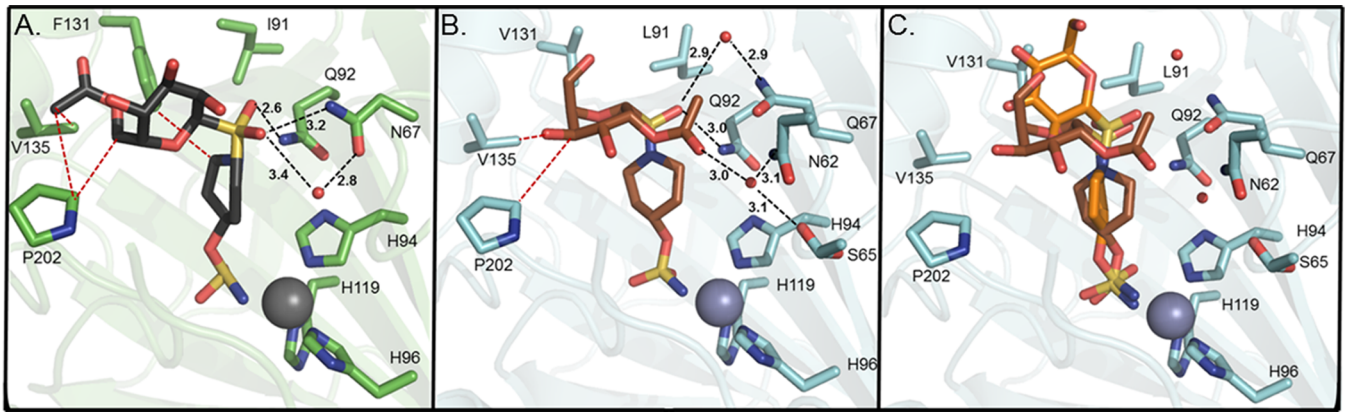

Figure 4. Compound **626** bound in the active site of both hCA II (PDB ID 4ZWI, green)[30] and the hCA IX-mimic (cyan) with specific residues labeled. (A) Specific interactions of compound **626** (black) with the active site of hCA II are shown with relative bond distances shown as black dotted lines with distances labeled (Å), hydrophobic interactions shown as red dotted lines, and water molecules shown as red spheres. (B) Specific interactions of compound **626** (brown) with the active site of the hCA IX-mimic are shown with relative bond distances shown as black dotted lines with distances labeled (Å), hydrophobic interactions shown as red dotted lines, and water molecules shown as red spheres. (C) Overlay of compound **626** with compound **5d** (PDB ID 4R59[21]) to show the change in relative position of the compound from its acetylated to its deacytlated form with active site residues labeled. Figure was made using PyMol.[38]

induces full displacement of the ordered water network (Figure 3A). There is a clear difference in the orientation of compound **625** in the active site of hCA II compared to the hCA IX-mimic (Figure 3), which results in a weakening of hydrogen bonding between Gln92 and His64 as determined by an increase in relative bond distances (Figure 3B). The acetyl group at position 6 of the glucose ring in compound **625**, as it is bound in the hCA II active site, shows a direct interaction with the amide of Asn62 (hydrogen bond distance of 2.9 Å) that most likely contributes to the compounds stabilization. Compound **625** also shows hydrophobic interactions in hCA II that are similar to the hCA IX-mimic via interactions with Val121, Phe131, and Leu198 (Figure 3B). However, there is no observable interaction with the residue at position 91 (Ile in hCA II) unlike in the hCA IX-mimic, which also might contribute to the decrease in the affinity of compound **625** for hCA II. Most likely, the major contributing factor to the increased hydrophobic interactions and stronger hydrogen bonding in the hCA IX active site versus hCA II is the replacement of Phe131 (hCA II) with Val131 (hCA IX) (Figure 3). The removal of the aromatic ring in the active site of hCA IX allows the bulky compound to more readily "fit" in the enzymes active site via a reduction in steric hindrance. This is probably the reason compound **625** is even less potent for hCA I (K_i = 9500 nM, Table 1), which has a phenylalanine in its active site at position 91 and a tyrosine at position 204 (both occupy positions in the *selective pocket*). In addition, the allowance for compound **625** to readily interact with Leu91 in the hCA IX-mimic is also predicted to contribute favorable to its selective inhibition for the enzyme.

A similar phenomenon is observed with compound **625** in both hCA II and the hCA IX-mimic to that of **623**, where there is clear ester hydrolysis of the acetyl groups of the glucose moiety (Supporting Information Figure S2B,C). In this particular case, there is complete ester hydrolysis of all acetyl groups of the glucose moiety of compound **625** as it resides in the active site of the hCA IX-mimic causing the compound to form its deacetylated counterpart, compound **625′** (Figures S1,S2B). In hCA II, all but the acetyl group at position 6 of the glucose ring are cleaved. The acetyl group in fact allows for a key interaction to form with Asn62 in the hCA II active site that most likely helps the compound to bind to the enzyme (Figure 3B). It is unknown if the arrangement of a specific acetyl group on the glucose ring plays a role in determining the molecular propensity for its cleavage and how this translates to the determined K_i values of the perceived acetylated compound. Interestingly, this phenomenon occurs after the enzymes (both hCA II and the hCA IX-mimic) have crystallized and compounds were soaked into them (see Experimental Section).

The X-ray crystal structure of the hCA IX-mimic in complex with compound **626** was determined (Table 2). Compound **626** shows selective binding for hCA IX (K_i = 2 nM) that is ~130-fold that of hCA II (K_i = 265 nM) (Table 1). Previously, it has been shown that compound **626** binds in the active site of hCA II and coordinates to the active site zinc via the sulfamate moiety similar to the other compounds of this series (Figure 4A).[30] Also, similar to the previous compounds, there is total displacement of the ordered water network in the enzyme's active site (Figure 4A). These two attributes are also observed as the compound resides in the active site of the hCA IX-mimic (Figure 4A,B). Key interactions of compound **626** with hCA II occur via strong hydrogen bonding (distance = 2.6 Å) between the O of the sulfonyl linker and the amide on the side chain of Gln92 and also in coordination with a solvent molecule and the hydroxyl of the side chain of Asn67 (Figure 4A). In addition, compound **626** exhibits hydrophobic interactions with the acetyl group (position 6 of the glucose ring) and Pro202 and the six-membered piperidine ring and Phe131 (Figure 4A). In likeness to what has been previously observed, there is ester hydrolysis of acetyl groups at positions 2, 3, and 4 of the glucose ring of compound **626** by hCA II.

Key interactions of compound **626** with the active site of the hCA IX-mimic are observed via hydrogen bonds that are formed from coordination of the O of the sulfonyl linker, the amide of the side chain of Gln92, a solvent molecule, and the amide side chain of Gln67 (Figure 4B). Similarly, there are hydrogen bonds formed between the carbonyl oxygen of the acetyl group (position 2 of the glucose ring) and a solvent molecule that is coordinated between the hydroxyl of the side chain of Ser65 and the amide side chain of Asn62 (Figure 4A). Important hydrophobic interactions appear to occur between the carbons of the glucose ring, Val135 and Pro202 (Figure

DOI: 10.1021/acs.jmedchem.5b00845
J. Med. Chem. 2015, 58, 6630−6638

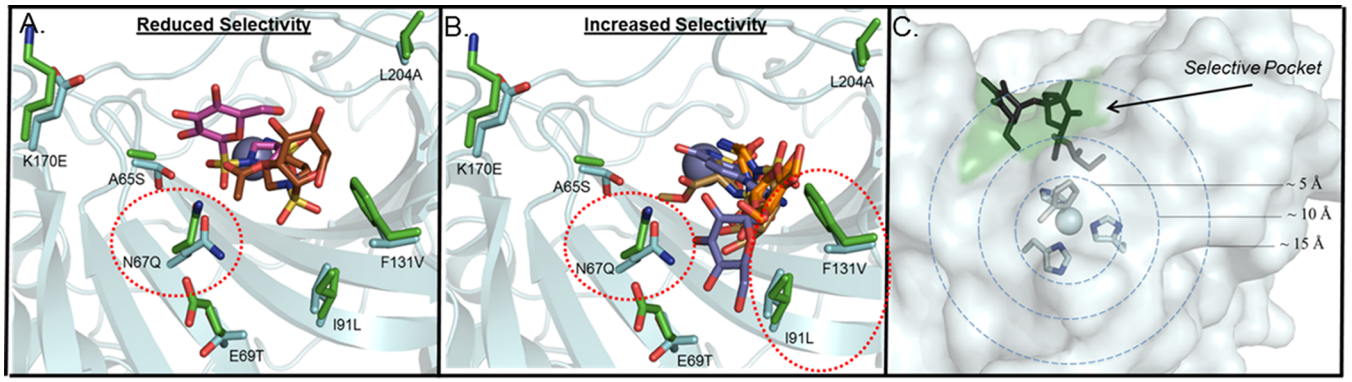

Figure 5. Active-site of the hCA IX-mimic with "mapped" interaction sites for inhibitor selectivity. (A) Compounds **5e** (pink, PDB ID 4R5A[21]) and **626** (brown) overlaid in the hCA IX-mimic active site. Both compounds show a reduced selectivity profile for hCA IX over the other off-target hCAs compared to other compounds in the sulfamate series. Labeled are active site residue substitutions from hCA II (green) to hCA IX (cyan). Highlighted are key residues that form important hydrophilic interactions that increase inhibitor selectivity for hCA IX. B). Compounds **5d** (orange, PDB ID 4R59[21]), **625** (tan), and a saccharin-conjugated hCA IX inhibitor (purple, PDB ID 4RIU[28]) that exhibited the highest hCA IX selectivity overlaid in the active site of the hCA IX-mimic (cyan) with substituted residues from hCA II labeled (green). Highlighted are the key interactions that induce the high hCA IX selective inhibition. (C) Cross-section of the CA active site marking distance shells relative to the active site zinc. The *selective pocket* is highlighted in green. Overlays of 4-methylimidazole (light-gray, PDB ID 4HEY[41]), glycerol (dark-gray, PDB ID 3HS4[42]), and sucrose (black, PDB ID 4YWP[31]), which correspond to chemical fragments of *none*, *least*, and *most* selective, respectively. Figure was made using PyMol.[38]

4B). The selectivity for this compound for hCA IX versus hCA II most likely occurs via the replacement of Asn for Gln at position 67 (from hCA II to hCA IX, respectively) which allows for the formation of additional hydrogen bonding to occur. The absence of Phe131 (Val in hCA IX) in the active site of hCA IX most likely allows for a reduction in steric hindrance (similar to that observed with compound **625**), allowing for a more favorable conformation of compound **626** in the active site of hCA IX. In addition, this allows for the induction of hydrophobic interactions with the glucose ring moiety contributing to the compounds stabilization in the active site.

Ester hydrolyzing events also have been observed to occur with compound **626** in complex with both hCA II and the hCA IX-mimic. Interestingly, ester hydrolysis of the acetylglucose ring occur at different positions between each enzyme such that hydrolysis of all acetyl groups except for that at position 6 has been observed in hCA II, and all but the acetyl at position 2 have been hydrolyzed in the hCA IX-mimic (Figure 4A,B). Currently, the ester hydrolysis of acetyl groups on compound **626** appears random based on our limited data, and there is no observable trend that indicates which positions of the acetyl groups on the glucose ring are more likely to undergo ester hydrolysis. When compound **626** undergoes full ester hydrolysis to become compound **626′** (Supporting Information Figure S1), it has previously been shown to display a very high selectivity ratio for hCA IX over hCA II (>2000-fold).[21] There is, however, a increase in observed K_i value between **626** and **626′** in hCA IX (2 and 10 nM for **626** and **626′**, respectively). This most likely is a result of a loss of interactions between acetyl groups from compound **626** with the enzymes active site as previously discussed (Figure 4C). However, it should be noted this decrease in affinity is slight, and it is more significant to note that when compound **626** is hydrolyzed to form compound **626′**, there is a substantial reduction in inhibition of hCA II, which is highly favorable.[21] This is reiterated in the failure of compound **626′** to readily form a complex with hCA II as noted by Moeker et al.[21]

Map of the hCA IX Active Site for Isoform Specific Inhibition. By summarizing observed binding modalities from each enzyme/inhibitor complex shows that an isoform selective hCA IX inhibitor must exploit residues in the CA *selective pocket* in order to achieve desired specificity. Using the current structural data within our model system of the hCA IX active site (via the hCA IX-mimic), in combination with previously published results, it is possible to map out key attributes of the hCA IX active site to exploit for isoform specific inhibition of the enzyme.[21,28,31] It has been determined that the least selective inhibitors utilize mostly hydrophilic interactions in the hCA active site (Figure 5A). The most important interaction in the hydrophilic pocket appears to be with Gln67 in the hCA IX active site, as this forms stabilizing hydrogen bonding networks that are not present in the hCA II active site. However, it is clearly evident that the most selective compounds for hCA IX inhibition form interactions with residues in the enzymes hydrophobic pocket. We predict the reason for this is the absence of bulky residues in the hCA IX active site such as Phe131 (hCA II) and Phe91 and Tyr204 (hCA I) that reduce the steric hindrance of the compound to (1) more freely enter the active site and (2) reside in the active site in a favorable conformation that allows for interactions with residues in the hydrophobic pocket, such as Leu91, which appears to form important interactions to induce selectivity (Figure 5B). As such, Phe131 (hCA II) and Phe91 and Tyr204 (hCA I) can be referred to as substrate/compound "steric-blocker" residues in human carbonic anhydrases. Lastly, the relative distance a compounds "tail" region is located relative to the ZBG has been shown to be important for selective inhibition. This is also apparent when comparing previously determined structures of chemical fragments or compounds that show either high selectivity for hCA IX or relatively ubiquitous inhibition for all hCAs. One such case is recent data that suggests sucrose will selectively bind to hCA IX over hCA II (K_d = 150 mM for hCA IX and K_d = 450 mM for hCA II).[31] Sucrose binds directly in the *selective pocket* of hCA IX which is ~12 Å from the catalytic zinc (Figure 5C). Alternatively, compounds that are not selective form primary interactions that are below or above the *selective pocket* (Figure 2B,C). In summary, these

DOI: 10.1021/acs.jmedchem.5b00845
J. Med. Chem. 2015, 58, 6630−6638

observations provide the necessary parameters that must be considered when designing hCA IX selective inhibitors.

CONCLUSIONS

Previously, it has been determined that the series of carbohydrate-based sulfamates and their acetylated counterparts are excellent inhibitors of hCA IX and hCA XII and highly selective for these enzymes over the off-target hCA I and II.[23] Here, we expand on these findings with novel structural information that, when coupled with our previous results, have allowed us to fully map the active site of hCA IX and pinpoint key interactions that are important for inhibitor selectivity. This includes taking advantage of key residues of the enzyme's *selective pocket* via designing linker regions of compounds with specific lengths to allow the compound's "tail" regions to reach the residues of the *selective pocket* located ∼12 Å from the catalytic zinc. In addition, it is apparent that designing more bulky compounds induces selective inhibition for hCA IX because its active site is perceived to be more "open" with the absence of several aromatic residues, termed hCA substrate/compound "steric-blocker" residues in the *selective pocket* of the enzyme. This essentially allows inhibitors to form highly favorable hydrophobic interactions that significantly increase their affinity for hCA IX. In summary, our findings have for the first time provided a molecular outline of the enzymes active site that will be advantageous for not only determining useful SARs of known hCA inhibitors but also provide the framework to design novel compounds that will be highly potent and selective for hCA IX, ultimately leading to novel therapies for the treatment of several cancers.

EXPERIMENTAL SECTION

Protein Expression, Purification, and CA IX-Mimic Design. The hCA IX-mimic construct was engineered by site-directed mutagenesis of residues in the active site of hCA II to residues unique to hCA IX, such that the active site of the hCA IX-mimic is analogous to wild-type hCA IX.[32] The advantage of the hCA IX-mimic is that it is extremely stable and readily crystallizes, allowing direct structural insight into hCA II versus hCA IX inhibitor binding with a range of novel small molecules.[21,28] Wild-type hCA II and hCA IX-mimic were expressed and purified using BL21DE3 competent cells as described by Mahon et al.[28] The hCA IX-mimic used for this study was designed and engineered previously by Genis et al.[32] (containing two active site mutations) and reconstructed by Pinard et al.[33] (to contain seven active site mutations). Utilization of the hCA IX-mimic was similar to that described by Pinard et al., Mahon et al., and Moeker et al.[21,28,33] Active site mutations in the hCA IX-mimic include: A65S, N67Q, E69T, I91L, F131V, K170E, and L204A. Purity of each enzyme was estimated by SDS-PAGE and staining with commassie. Concentrations were determined by UV/vis spectroscopy and measured at 22 and 25 mg/mL for the hCA IX-mimic and hCA II, respectively.

X-ray Crystallography. Purified hCA II and hCA IX-mimic were crystallized in 1.6 M Na-citrate, 50 mM Tris, pH 7.8, using hanging drop vapor diffusion.[21,28,33] Crystals for both enzymes were observed after 5 days. Stock solutions of each compound were made using a 100% dimethyl sulfoxide (DMSO) solution and to a final concentration of ∼50 mM for each. Sock solutions of compounds were diluted 1:1 (50% DMSO at ∼25 mM) in deionized water prior to soaking with protein crystals. Crystals were than soaked with the desired compound solution 24 h prior to data collection. Diffraction data were collected "in-house" using an RU-H3R rotating Cu anode (λ = 1.5418 Å) operating at 50 kV and 22 mA utilizing an R-Axis IV^{+2} image plate detector (Rigaku, USA). Each data set was processed using HKL2000.[34] All data sets were scaled to a $P2_1$ space group with statistics summarized in Table 1. Initial phases for each data set were determined using molecular replacement methods using PDB 3KS3[27] as a search model. Molecular replacement, model refinements, and generation of ligand restraint files were performed using Phenix.[35] Models for ligand−protein complexes and PDB files for ligands were generated using Coot.[36,37] Coot[36] was also used to determine bond lengths and angles used for analysis. Figures were generated using PyMol.[38]

CA Inhibition Assay. An Applied Photophysics stopped-flow instrument was used for assaying the CA-catalyzed CO_2 hydration activity.[39] IC_{50} values were obtained from dose−response curves working at seven different concentrations of test compound; by fitting the curves using PRISM (www.graphpad.com) and nonlinear least-squares methods, values represent the mean of at least three different determinations as described by us previously.[40] The inhibition constants (K_i) were then derived by using the Cheng−Prusoff equation, as follows: $K_i = IC_{50}/(1 + [S]/K_m)$ where [S] represents the CO_2 concentration at which the measurement was carried out and K_m the concentration of substrate at which the enzyme activity is at half-maximal. All enzymes used were recombinant, produced in *Escherichia coli* as reported earlier.[40] The concentrations of enzymes used in the assay were: HCA I, 10.4 nM; HCA II, 8.3 nM; HCA IX, 8.0 nM; and HCA XII, 12.4 nM.

ASSOCIATED CONTENT

Supporting Information

The Supporting Information is available free of charge on the ACS Publications website at DOI: 10.1021/acs.jmedchem.5b00845.

Additional figures and chemistry (PDF)
Molecular formula strings (CSV)

Accession Codes

Coordinates and structure factors for all structures have been deposited to the PDB with the following accession codes: 4ZWX, 4ZWY, 4ZWZ, 4ZX0, and 4ZX1.

AUTHOR INFORMATION

Corresponding Author

*Phone: 352-392-5696. Fax: 352-392-3422. E-mail: rmckenna@ufl.edu.

Notes

The authors declare no competing financial interest.

ACKNOWLEDGMENTS

This research was financed by the Australian Research Council (grant nos. DP110100071, FT10100185 to S.-A.P.), two EU grants of the seventh framework program (Metoxia and Dynano projects to C.T.S.), and R.M. was supported in part by the National Institutes of Health grant CA165284.

ABBREVIATIONS USED

hCA, human carbonic anhydrase; K_i, inhibition constant; ZBG, zinc binding group

REFERENCES

(1) Höckel, M.; Vaupel, P. Tumor Hypoxia: Definitions and Current Clinical, Biologic, and Molecular Aspects. *J. Natl. Cancer Inst.* **2001**, *93* (4), 266−276.

(2) Sadri, N.; Zhang, P. Hypoxia-Inducible Factors: Mediators of Cancer Progression; Prognostic and Therapeutic Targets in Soft Tissue Sarcomas. *Cancers* **2013**, *5* (2), 320−333.

(3) Warburg, O.; Geissler, A. W.; Lorenz, S. On Growth of Cancer Cells in Media in which Glucose is Replaced by Galactose]. *Hoppe-Seyler's Z. Physiol. Chem.* **1967**, *348* (12), 1686−1687.

DOI: 10.1021/acs.jmedchem.5b00845
J. Med. Chem. 2015, 58, 6630−6638

(4) Racker, E. Warburg Effect Revisited. *Science* **1981**, *213* (4514), 1313.
(5) DeBerardinis, R. J.; Lum, J. J.; Hatzivassiliou, G.; Thompson, C. B. The Biology of Cancer: Metabolic Reprogramming Fuels Cell Growth and Proliferation. *Cell Metab.* **2008**, *7* (1), 11−20.
(6) Mahon, B. P.; McKenna, R. Regulation and Role of Carbonic Anhydrase IX and Use as a Biomarker and Therapeutic Target in Cancer. *Res. Trends Curr. Top. Biochem. Res.* **2013**, *15*, 1−21.
(7) Mahon, B. P.; Pinard, M. A.; McKenna, R. Targeting Carbonic Anhydrase IX Activity and Expression. *Molecules* **2015**, *20* (2), 2323−2348.
(8) Chiche, J.; Ilc, K.; Laferriere, J.; Trottier, E.; Dayan, F.; Mazure, N. M.; Brahimi-Horn, M. C.; Pouyssegur, J. Hypoxia-Inducible Carbonic Anhydrase IX and XII Promote Tumor Cell Growth by Counteracting Acidosis through the Regulation of the Intracellular pH. *Cancer Res.* **2009**, *69* (1), 358−368.
(9) Supuran, C. T. Carbonic Anhydrases: Novel Therapeutic Applications for Inhibitors and Activators. *Nat. Rev. Drug Discovery* **2008**, *7* (2), 168−181.
(10) Lock, F. E.; McDonald, P. C.; Lou, Y.; Serrano, I.; Chafe, S. C.; Ostlund, C.; Aparicio, S.; Winum, J.-Y.; Supuran, C. T.; Dedhar, S. Targeting Carbonic Anhydrase IX Depletes Breast Cancer Stem Cells within the Hypoxic Niche. *Oncogene* **2013**, *32* (44), 5210−5219.
(11) Lou, Y.; McDonald, P. C.; Oloumi, A.; Chia, S.; Ostlund, C.; Ahmadi, A.; Kyle, A.; Auf dem Keller, U.; Leung, S.; Huntsman, D.; Clarke, B.; Sutherland, B. W.; Waterhouse, D.; Bally, M.; Roskelley, C.; Overall, C. M.; Minchinton, A.; Pacchiano, F.; Carta, F.; Scozzafava, A.; Touisni, N.; Winum, J.-Y.; Supuran, C. T.; Dedhar, S. Targeting Tumor Hypoxia: Suppression of Breast Tumor Growth and Metastasis by Novel Carbonic Anhydrase IX Inhibitors. *Cancer Res.* **2011**, *71* (9), 3364−3376.
(12) Alterio, V.; Hilvo, M.; Di Fiore, A.; Supuran, C. T.; Pan, P.; Parkkila, S.; Scaloni, A.; Pastorek, J.; Pastorekova, S.; Pedone, C.; Scozzafava, A.; Monti, S. M.; De Simone, G. Crystal Structure of the Catalytic Domain of the Tumor-Associated Human Carbonic Anhydrase IX. *Proc. Natl. Acad. Sci. U. S. A.* **2009**, *106* (38), 16233−16238.
(13) De Simone, G.; Supuran, C. T. Carbonic Anhydrase IX: Biochemical and Crystallographic Characterization of a Novel Antitumor Target. *Biochim. Biophys. Acta, Proteins Proteomics* **2010**, *1804* (2), 404−409.
(14) Brennan, D. J.; Jirstrom, K.; Kronblad, A.; Millikan, R. C.; Landberg, G.; Duffy, M. J.; Rydén, L.; Gallagher, W. M.; O'Brien, S. L. CA IX Is an Independent Prognostic Marker in Premenopausal Breast Cancer Patients with One to Three Positive Lymph Nodes and a Putative Marker of Radiation Resistance. *Clin. Cancer Res.* **2006**, *12* (21), 6421−6431.
(15) Chia, S. K.; Wykoff, C. C.; Watson, P. H.; Han, C.; Leek, R. D.; Pastorek, J.; Gatter, K. C.; Ratcliffe, P.; Harris, A. L. Prognostic Significance of a Novel Hypoxia-Regulated Marker, Carbonic Anhydrase IX, in Invasive Breast Carcinoma. *J. Clin. Oncol.* **2001**, *19* (16), 3660−3668.
(16) Liao, S.-Y.; Lerman, M. I.; Stanbridge, E. J. Expression of Transmembrane Carbonic Anhydrases, CAIX and CAXII, in Human Development. *BMC Dev. Biol.* **2009**, *9* (1), 22.
(17) McDonald, P. C.; Winum, J.-Y.; Supuran, C. T.; Dedhar, S. Recent Developments in Targeting Carbonic Anhydrase IX for Cancer Therapeutics. *Oncotarget* **2012**, *3* (1), 84−97.
(18) Frost, S. C.; McKenna, R. *Carbonic Anhydrase Mechanism, Regulation, Links to Disease, and Industrial Applications*; Springer: Dordrecht, The Netherlands, 2014.
(19) Pinard, M. A.; Mahon, B. P.; McKenna, R. Probing the Surface of Human Carbonic Anhydrase for Clues Towards the Design of Isoform Specific Inhibitors. *BioMed Res. Int.* **2015**, 453543.
(20) Aggarwal, M.; Kondeti, B.; McKenna, R. Insights towards Sulfonamide Drug Specificity in A-Carbonic Anhydrases. *Bioorg. Med. Chem.* **2013**, *21* (6), 1526−1533.
(21) Moeker, J.; Mahon, B. P.; Bornaghi, L. F.; Vullo, D.; Supuran, C. T.; McKenna, R.; Poulsen, S.-A. Structural Insights into Carbonic Anhydrase IX Isoform Specificity of Carbohydrate-Based Sulfamates. *J. Med. Chem.* **2014**, *57* (20), 8635−8645.
(22) Lopez, M.; Trajkovic, J.; Bornaghi, L. F.; Innocenti, A.; Vullo, D.; Supuran, C. T.; Poulsen, S.-A. Design, Synthesis, and Biological Evaluation of Novel Carbohydrate-Based Sulfamates as Carbonic Anhydrase Inhibitors. *J. Med. Chem.* **2011**, *54* (5), 1481−1489.
(23) Carroux, C. J.; Rankin, G. M.; Moeker, J.; Bornaghi, L. F.; Katneni, K.; Morizzi, J.; Charman, S. A.; Vullo, D.; Supuran, C. T.; Poulsen, S.-A. A Prodrug Approach toward Cancer-Related Carbonic Anhydrase Inhibition. *J. Med. Chem.* **2013**, *56* (23), 9623−9634.
(24) Lopez, M.; Vu, H.; Wang, C. K.; Wolf, M. G.; Groenhof, G.; Innocenti, A.; Supuran, C. T.; Poulsen, S.-A. Promiscuity of Carbonic Anhydrase II. Unexpected Ester Hydrolysis of Carbohydrate-Based Sulfamate Inhibitors. *J. Am. Chem. Soc.* **2011**, *133* (45), 18452−18462.
(25) Steiner, H.; Lindskog, S. Effects of High Concentrations of Salt on the Esterase Activity of Human Carbonic Anhydrase. *FEBS Lett.* **1972**, *24* (1), 85−88.
(26) Mikulski, R.; West, D.; Sippel, K. H.; Avvaru, B. S.; Aggarwal, M.; Tu, C.; McKenna, R.; Silverman, D. N. Water Networks in Fast Proton Transer During Catalysis by Human Carbonic Anhydrase II. *Biochemistry* **2013**, *52* (1), 125.
(27) Avvaru, B. S.; Kim, C. U.; Sippel, K. H.; Gruner, S. M.; Agbandje-McKenna, M.; Silverman, D. N.; McKenna, R. A Short, Strong Hydrogen Bond in the Active Site of Human Carbonic Anhydrase II. *Biochemistry* **2010**, *49* (2), 249.
(28) Mahon, B. P.; Hendon, A. M.; Driscoll, J. M.; Rankin, G. M.; Poulsen, S.-A.; Supuran, C. T.; McKenna, R. Saccharin: A Lead Compound for Structure-Based Drug Design of Carbonic Anhydrase IX Inhibitors. *Bioorg. Med. Chem.* **2015**, *23* (4), 849−854.
(29) Fisher, Z.; Hernandez Prada, J. A.; Tu, C.; Duda, D.; Yoshioka, C.; An, H.; Govindasamy, L.; Silverman, D. N.; McKenna, R. Structural and Kinetic Characterization of Active-Site Histidines as a Proton Shuttle in Catalysis by Human Carbonic Anhydrase II. *Biochemistry* **2005**, *44* (4), 1097.
(30) Mahon, B. P.; Lomelino, C. L.; Salguero, A. L.; Driscoll, J. M.; Pinard, M. A.; McKenna, R. Observations of Surface Lysine Acetylation in Human Carbonic Anhydrase Expressed in Escherichia Coli. 2015, unpublished results.
(31) Pinard, M. A.; Aggarwal, M.; Mahon, B. P.; Tu, C.; McKenna, R. *Acta Crystallogr. Sect. F: Struct. Biol. Commun.* **2015**.
(32) Genis, C.; Sippel, K. H.; Case, N.; Cao, W.; Avvaru, B. S.; Tartaglia, L. J.; Govindasamy, L.; Tu, C.; Agbandje-McKenna, M.; Silverman, D. N.; Rosser, C. J.; McKenna, R. Design of a Carbonic Anhydrase IX Active-Site Mimic to Screen Inhibitors for Possible Anticancer Properties. *Biochemistry* **2009**, *48* (6), 1322.
(33) Pinard, M. A.; Boone, C. D.; Rife, B. D.; Supuran, C. T.; McKenna, R. Structural Study of Interaction between Brinzolamide and Dorzolamide Inhibition of Human Carbonic Anhydrases. *Bioorg. Med. Chem.* **2013**, *21* (22), 7210−7215.
(34) Otwinowski, Z.; Minor, W. Processing of X-Ray Diffraction Data Collected in Oscillation Mode. In *Methods in Enzymology*; Elsevier: Amsterdam, 1997; Vol. *276*, pp 307−326.
(35) Adams, P. D.; Afonine, P. V.; Bunkóczi, G.; Chen, V. B.; Echols, N.; Headd, J. J.; Hung, L.-W.; Jain, S.; Kapral, G. J.; Grosse Kunstleve, R. W.; McCoy, A. J.; Moriarty, N. W.; Oeffner, R. D.; Read, R. J.; Richardson, D. C.; Richardson, J. S.; Terwilliger, T. C.; Zwart, P. H. The Phenix Software for Automated Determination of Macromolecular Structures. *Methods* **2011**, *55* (1), 94−106.
(36) Emsley, P.; Cowtan, K. Coot: Model-Building Tools for Molecular Graphics. *Acta Crystallogr., Sect. D: Biol. Crystallogr.* **2004**, *60*, 2126−2132.
(37) Debreczeni, J. É.; Emsley, P. Handling Ligands with Coot. *Acta Crystallogr., Sect. D: Biol. Crystallogr.* **2012**, *68*, 425−430.
(38) *The PyMOL Molecular Graphics System*, version 1.2r3pre; Schrödinger, LLC, LLC.
(39) Khalifah, R. G. The Carbon Dioxide Hydration Activity of Carbonic Anhydrase. I. Stop-Flow Kinetic Studies on the Native Human Isoenzymes B and C. *J. Biol. Chem.* **1971**, *246* (8), 2561−2573.

DOI: 10.1021/acs.jmedchem.5b00845
J. Med. Chem. 2015, 58, 6630−6638

(40) Ilies, M. A.; Vullo, D.; Pastorek, J.; Scozzafava, A.; Ilies, M.; Caproiu, M. T.; Pastorekova, S.; Supuran, C. T. Carbonic Anhydrase Inhibitors. Inhibition of Tumor-Associated Isozyme IX by Halogenosulfanilamide and Halogenophenylaminobenzolamide Derivatives. *J. Med. Chem.* **2003**, *46* (11), 2187−2196.
(41) Aggarwal, M.; Kondeti, B.; Tu, C.; Maupin, C. M.; Silverman, D. N.; McKenna, R. Structural Insight into Activity Enhancement and Inhibition of H64A Carbonic Anhydrase II by Imidazoles. *IUCrJ* **2014**, *1* (2), 129−135.
(42) Sippel, K. H.; Robbins, A. H.; Domsic, J.; Genis, C.; Agbandje-McKenna, M.; McKenna, R. High-Resolution Structure of Human Carbonic Anhydrase II Complexed with Acetazolamide Reveals Insights into Inhibitor Drug Design. *Acta Crystallogr., Sect. F: Struct. Biol. Cryst. Commun.* **2009**, *65* (10), 992−995.

DOI: 10.1021/acs.jmedchem.5b00845
J. Med. Chem. 2015, 58, 6630−6638